

Fission-Excitation Functions in Interactions of ^{11}B , ^{12}C , ^{14}N , and ^{19}F with Various Targets[†]

Torbjørn Sikkeland,* Jack E. Clarkson,‡ Naftali H. Steiger-Shafir,§ and V. E. Viola ||
Lawrence Radiation Laboratory, University of California, Berkeley, California 94720
 (Received 29 June 1970)

Fission cross sections for the systems $^{169}\text{Tm} + ^{11}\text{B}$, $^{175}\text{Lu} + ^{11}\text{B}$, and ^{12}C , $^{174}\text{Y} + ^{12}\text{C}$, $^{182}\text{W} + ^{12}\text{C}$, $^{165}\text{Ho} + ^{14}\text{N}$, and $^{159}\text{Tb} + ^{19}\text{F}$ have been measured for heavy-ion bombarding energies up to 10.4 MeV per nucleon. The experimental technique consisted of counting coincident fission-fragment pairs with two gold-surface-barrier silicon-diode detectors. For the above systems, fission takes place only in reactions in which a compound nucleus is formed between the incident projectile and the target nucleus. Values of the compound-nucleus cross sections for these reactions are estimated from other data in order to account for surface reactions which occur in heavy-ion bombardment. The difference between the cross section for compound-nucleus formation and that for fission is assumed to be equal to the cross section for neutron-evaporation products. The ratio of the fission cross section to that for neutron evaporation is then taken to be equal to $\langle \Gamma_f / \Gamma_n \rangle$, the ratio of the level widths for the two competing processes averaged over the various reaction channels. A theoretical fit to the $\langle \Gamma_f / \Gamma_n \rangle$ values is obtained for the low-energy region of the excitation function, where first-chance fission is highly probable. We find the ratio of the level-density parameter for fission to that for neutron emission to be 1.2 ± 0.1 , and values for the fission barrier to be in agreement with those predicted by Myers and Swiatecki.

I. INTRODUCTION

Measurements of fission-excitation functions constitute an important source of information concerning the probability of nuclear fission as a function of various nuclear parameters.¹ Analysis of fission-to-neutron-evaporation level-width ratios, Γ_f / Γ_n , derived from such data are useful in determining nuclear level-density parameters, fission-barrier heights, the dependence of fissionability on angular momentum, etc.² Investigations of this type have been performed for several combinations of bombarding ions and heavy target nuclides ($A > 200$), the results of which are summarized in Refs. 1 and 2.

The present work is primarily concerned with these aspects of the fission process when heavy ions are used as incident particles on light target nuclides in the rare-earth region and is a continuation of studies reported previously.³ A broad understanding of fission probabilities for heavy-ion-induced nuclear reactions is of particular concern at the present time in view of current efforts to synthesize superheavy elements near $Z = 114$ by means of such reactions. In addition a knowledge of trends in fission-barrier energetics as a function of atomic number Z and mass number A are useful in estimating the stability of such elements against spontaneous fission. In this work we have measured fission-excitation functions for a series of primarily even- Z compound nuclei using the projectiles ^{11}B , ^{12}C , ^{14}N , and ^{19}F and the targets ^{174}Yb

and ^{182}W (separated isotopically) and ^{159}Tb , ^{165}Ho , ^{169}Tm , and ^{175}Lu (naturally monoisotopic). In Ref. 3 these same targets were studied with ^{12}C , ^{16}O , and ^{20}Ne ions.

For heavy ions incident on targets heavier than tungsten ($Z = 74$), fission cross sections are nearly equal to the compound-nucleus formation cross section. For this reason it is not possible to obtain reliable Γ_f / Γ_n values without simultaneous measurement of both fission cross sections and neutron-evaporation cross sections. However, for the systems examined here and in Ref. 3, the fission cross section differs sufficiently from that for compound-nucleus formation that the neutron-evaporation cross section can be determined reliably from the difference between the calculated compound-nucleus formation cross section and the measured fission cross section (see below). The accuracy of this assumption is probably comparable to that for the experimental determination of total neutron-evaporation cross sections.

The experimental technique employed here is similar to that of Ref. 3. It consists of counting coincident fission-fragment pairs with two gold-surface-barrier silicon-diode detectors. The advantage of this method is that a fission event is not only identified by the energy of the fragments, but also by a coincidence requirement and by an angular correlation between the two fragments. The latter characteristic offers a convenient way of studying fission of targets lighter than lead and bismuth. In general such targets will have heavy-ele-

ment impurities such as lead, bismuth, and uranium that are difficult to eliminate. By proper positioning of the two detectors, one can minimize interference from fission of such impurities.

The theoretical analysis is somewhat different from that of Ref. 3. As will be described in Sec. IV, the average value for Γ_f/Γ_n , denoted $\langle \Gamma_f/\Gamma_n \rangle$, is obtained by averaging over Γ_f/Γ_n for individual l waves of the incoming ions. In Ref. 3, $\langle \Gamma_f/\Gamma_n \rangle$ was set equal to Γ_f/Γ_n for the average l wave of the compound-nucleus reactions that initiate fission. We shall also use a formula for Γ_f/Γ_n which contains angular momentum terms. The main purpose of the fitting process is to obtain values for the fission-barrier height.

II. EXPERIMENTAL PROCEDURE

We shall only give a brief account of the experimental arrangement, since it has been described in earlier publications.³⁻⁵ Heavy-ion beams were furnished by the Berkeley heavy-ion linear accelerator which accelerates ions to 10.4 MeV/nucleon. The beam was magnetically deflected through 30° before reaching the fission chamber. Lower energies were obtained by inserting weighed aluminum foils into the beam path. Northcliffe's range-energy curves for aluminum were used to estimate the resulting energy.⁶ Additionally, the ranges of the ions in emulsion were measured and from this the average energy and the energy spread could be evaluated.⁷ The average energies obtained with the two methods were generally in agreement at the highest energies, but differed by as much as 2 MeV at the lowest energies.

For convenience we used range-energy curves, the values of which we assigned an error of ± 2 MeV. The energy spreads, full width at half maximum were about 2% at full energy and increased very linearly with decreasing ion energy to about 5% at the lowest energies.

Before striking the target, the beam passed through two circular collimators 1.5 mm in diameter and 62 cm apart. The last collimator was 6 cm from the target. The beam current was collected in a Faraday cup arrangement, described previously³⁻⁵ and was converted to the number of particles striking the target with the aid of values for the equilibrium charge distributions for heavy ions passing through matter.⁸ Targets were made by vaporizing the metals onto 100- $\mu\text{g}/\text{cm}^2$ nickel films. Target thicknesses were about 200 $\mu\text{g}/\text{cm}^2$.

The silicon detectors were of the gold-surface-barrier type. They were mounted on movable arms with one of them in a permanent position at 90° to the beam. The angular position ψ of the second detector was varied to obtain the angular cor-

relation of fission events. Circular collimators were used for both detectors, each with a geometry of 1.4×10^{-3} sr. Measurement of the angular-correlation functions is important in these experiments in order to obtain the following information: (a) The relative contribution of fission induced by surface reactions to the total fission cross section; this is found to be a negligible effect for the targets used here.

(b) The angular position ψ of the most probable angle of coincidence with the 90° detector.

(c) The most probable value of the center-of-mass transformation parameter, χ^2_{mp} .

The latter parameter is defined as $\chi^2 = (V/\nu)^2$, where V is the velocity of the center of mass and ν is the velocity of the reaction product in the center-of-mass system.

The parameter χ^2_{mp} is related to the most probable angle of coincidence ψ by the relationship

$$\chi^2_{\text{mp}} = (1 + 4 \tan^2 \psi)^{-1}. \quad (1)$$

It is necessary to know this quantity in order to convert the laboratory angular distributions to the center-of-mass system for calculation of the total cross sections, as discussed below.

Measurement of the fission cross sections for the compound nuclei formed in these bombardments is complicated by the relatively low kinetic energies of the fragments. With semiconductor detectors it becomes difficult to obtain differential cross sections from such fragments because the fission events are not easily differentiated from background noise. This problem can be eliminated by counting coincident events between two detectors.³ In order to determine the number of fragments emitted at a given angle using this technique, it is essential that the complementary detector have a large enough geometry to catch all coincident fragments; i.e., it must record the integrated angular correlation.

Values for the absolute differential fission cross section at 90°, $\xi^0_{\text{abs}}(\pi/2)$, have previously been measured for ¹⁶O at 10.4 MeV/nucleon incident on the targets used in the present work.³ Using those values the total fission cross section, σ_f , at various ion energies, was then measured in the following way.

A low geometry detector (1.4×10^{-3} sr) was used to measure the relative differential fission cross section, $\xi(\pi/2)$, at 90° in the laboratory system at each bombarding energy. A large geometry detector (0.28 sr) was then placed at the angle $\bar{\psi}$, determined in the angular-correlation experiments. The counting efficiency of this arrangement was checked for the system ¹⁹⁷Au + 124-MeV ¹²C ions, where distinct single fragment spectra could be obtained. We found the value for coincidence count-

ing to be about 95% of the value obtained from counting with a single detector. Appropriate corrections for this loss in counting efficiency were then applied to the data.

Using the same geometry and target, the value for the same quantity, $\xi^0(\pi/2)$, was measured with ^{16}O ions at 10.4 MeV/nucleon. After proper transformation to the center-of-mass system of the fissioning nucleus, using values for the parameter χ^2_{mp} as defined above, values for σ_f were estimated from the expression

$$\sigma_f = 2\pi \frac{\xi^0_{\text{abs}}(\frac{1}{2}\pi)}{\xi^0(\frac{1}{2}\pi)} \xi(\frac{1}{2}\pi) \int_0^\pi \frac{\xi(\theta)}{\xi(\frac{1}{2}\pi)} \sin\theta d\theta, \quad (2)$$

where values for $\xi^0_{\text{abs}}(\frac{1}{2}\pi)$ were taken from Ref. 3.

The integral in Eq. (2) accounts for the angular distribution relative to 90° for the fission fragments. The actual fragment angular distributions could not be measured because of difficulties in obtaining good fragment spectra for angles near the beam axis. However, it is known that the angular distributions follow the $1/\sin\theta$ law up to about 15° of the beam axis.³ We have assumed the integral to be 0.95π at 10.4 MeV/nucleon and that it decreases linearly with ion energy to 0.85π at 6 MeV/nucleon bombarding energy. Errors introduced by this assumption are believed to be about 5%. (By errors we mean standard deviation.)

III. EXPERIMENTAL RESULTS

The fragment-fragment angular-correlation functions of all the systems studied here showed only

one peak. The positions of the peaks and the fact that they were symmetric clearly demonstrates that all fragments originate from compound-nucleus formation between the target and projectile. Such correlation functions have been discussed and analyzed in detail in Refs. 4 and 5.

Values for the fission cross section at various ion energies for the different systems are given in Tables I-III. In the same tables are also listed the ratio σ_f/σ_R , where σ_R is the total reaction cross section, and \bar{l}_R , the average angular momentum generated in the reaction. Values for σ_R and \bar{l}_R were calculated as follows:

$$\sigma_R = \sum_{l=0}^{\infty} \sigma_l, \quad \bar{l}_R = (\sum_{l=0}^{\infty} l\sigma_l)/\sigma_R, \quad (3)$$

where σ_l is the cross section for the l th partial wave and is given by

$$\sigma_l = \pi\lambda^2(2l+1)T_l. \quad (4)$$

Here λ is the de Broglie wavelength of the projectile and T_l is the transmission coefficient. In the calculation of T_l we used the parabolic approximation to the real part of the optical-model potential suggested by Thomas.⁹ Values for the parameters of this potential were taken from Viola and Sikkeland.¹⁰

Generally, the errors in the ratio σ_f/σ_R are about 10%. The data have also been corrected for energy spread in the beam. This correction becomes significant only in regions where the fission cross section changes rapidly with bombarding energy.

TABLE I. Values for σ_f , σ_f/σ_R , and \bar{l}_R at various laboratory ion energies, E_L , for the systems ($^{159}\text{Tb} + ^{19}\text{F}$) and ($^{165}\text{Ho} + ^{14}\text{N}$), where σ_f is the total experimental fission cross section and σ_R and \bar{l}_R are, respectively, the estimated total cross section and average angular momentum in the interaction.

$^{159}\text{Tb} + ^{19}\text{F}$				$^{165}\text{Ho} + ^{14}\text{N}$			
E_L (MeV)	\bar{l}_R (\hbar)	σ_f (mb)	σ_f/σ_R	E_L (MeV)	\bar{l}_R (\hbar)	σ_f (mb)	σ_f/σ_R
193.8	68.0	530	2.30×10^{-1}	145.3	50.5	241	1.10×10^{-1}
170.2	60.0	516	2.46×10^{-1}	140.0	48.7	192	8.97×10^{-2}
155.0	55.5	421	2.16×10^{-1}	134.5	47.0	183	8.88×10^{-2}
143.5	51.0	329	1.81×10^{-1}	122.5	43.0	109	5.71×10^{-2}
132.2	46.4	219	1.32×10^{-1}	115.7	40.7	68.9	3.81×10^{-2}
120.6	42.0	166	1.15×10^{-1}	109.5	38.4	37.0	2.18×10^{-2}
113.8	35.0	120	9.40×10^{-2}	105.9	37.0	30.0	1.83×10^{-2}
107.9	30.5	62.0	5.48×10^{-2}	102.7	35.6	19.7	1.26×10^{-2}
101.1	28.0	28.8	3.10×10^{-2}	102.2	35.4	17.7	1.13×10^{-2}
94.2	26.0	8.0	1.13×10^{-2}	98.7	34.0	11.2	7.57×10^{-3}
87.0	19.1	1.4	3.4×10^{-3}	96.0	32.7	6.9	4.9×10^{-3}
				95.2	32.2	7.9	5.6×10^{-3}
				91.4	30.4	4.1	3.2×10^{-3}
				91.1	30.2	4.2	3.3×10^{-3}
				88.0	28.6	3.1	2.6×10^{-3}
				87.4	28.2	1.5	1.3×10^{-3}
				83.2	25.8	0.4	3.9×10^{-4}

TABLE II. Values for σ_f , σ_f/σ_R , and \bar{l}_R at various laboratory ion energies, E_L , for the systems ($^{169}\text{Tm} + ^{11}\text{B}$) and ($^{175}\text{Lu} + ^{11}\text{B}$) where σ_f is the total experimental fission cross section, and σ_R and \bar{l}_R are, respectively, the estimated total cross section and average angular momentum in the interaction.

$^{169}\text{Tm} + ^{11}\text{B}$				$^{175}\text{Lu} + ^{11}\text{B}$			
E_L (MeV)	\bar{l}_R (\hbar)	σ_f (mb)	σ_f/σ_R	E_L (MeV)	\bar{l}_R (\hbar)	σ_f (mb)	σ_f/σ_R
114.4	41.0	74.8	3.28×10^{-2}	114.4	41.2	134	5.80×10^{-2}
108.6	39.5	60.0	2.70×10^{-2}	110.0	39.7	101	4.51×10^{-2}
105.8	38.5	50.9	2.31×10^{-2}	105.7	38.5	71.9	3.34×10^{-2}
102.6	37.5	47.3	2.19×10^{-2}	101.2	37.0	58.6	2.79×10^{-2}
96.5	35.5	26.2	1.28×10^{-2}	96.6	35.5	31.4	1.53×10^{-2}
89.8	33.0	12.5	6.47×10^{-3}	93.5	34.5	26.4	1.32×10^{-2}
86.4	32.0	9.9	5.27×10^{-3}	88.4	32.6	15.3	8.05×10^{-3}
82.9	30.5	5.5	3.0×10^{-3}	83.3	30.7	6.6	3.7×10^{-3}
81.0	30.0	4.5	2.6×10^{-3}	79.6	29.3	4.7	2.8×10^{-3}
77.8	28.5	4.3	2.6×10^{-3}	71.6	25.7	1.7	1.2×10^{-3}
73.4	27.0	1.5	9.5×10^{-4}	69.6	24.8	0.9	7.0×10^{-4}
71.3	26.0	1.2	8.1×10^{-4}				

IV. DISCUSSION

A. Experimental $\langle \Gamma_f/\Gamma_n \rangle$ Values

As pointed out in the previous section, fission takes place only from reactions where a compound nucleus is formed between the bombarding ion and the targets studied in this work. In this case the initial compound nuclei in each reaction studied here all have the same nucleonic composition and excitation energy. The angular momentum distribution is a function of the incident heavy ion and hence varies from one compound nucleus to another.

The value of Γ_f/Γ_n for a system with a particular angular momentum l is denoted here as $(\Gamma_f/\Gamma_n)_l$ and that obtained by averaging over all l waves in the reaction is the average level width ratio $\langle \Gamma_f/\Gamma_n \rangle$.

In the region where the probability for fission is increasing rapidly with excitation energy, the experimental value of $\langle \Gamma_f/\Gamma_n \rangle$ can be approximated by the expression

$$\langle \Gamma_f/\Gamma_n \rangle = \sigma_f / (\sigma_{\text{CN}} - \sigma_f), \quad (5)$$

where σ_{CN} is the formation cross section for com-

TABLE III. Values for σ_f , σ_R , and \bar{l}_R at various laboratory ion energies, E_L , for ^{12}C ions incident on ^{174}Yb , ^{175}Lu , and ^{182}W where σ_f is the total experimental fission cross section, and σ_R and \bar{l}_R are, respectively, the estimated total cross section and average angular momentum in the interaction.

E_L (MeV)	$^{174}\text{Yb} + ^{12}\text{C}$			$^{175}\text{Lu} + ^{12}\text{C}$			$^{182}\text{W} + ^{12}\text{C}$		
	\bar{l}_R (\hbar)	σ_f (mb)	σ_f/σ_R	\bar{l}_R (\hbar)	σ_f (mb)	σ_f/σ_R	\bar{l}_R (\hbar)	σ_f (mb)	σ_f/σ_R
124.6	43.1	106.	4.91×10^{-2}	43.0	241	1.12×10^{-1}	43.0	752	3.58×10^{-1}
120.2	42.0	93.1	4.43×10^{-2}	41.9	220	1.05×10^{-1}	41.8	745	3.61×10^{-1}
116.3	40.8	69.8	3.39×10^{-2}	40.5	178	8.77×10^{-2}	40.2	612	3.06×10^{-1}
111.8	39.4	48.6	2.45×10^{-2}	39.1	147	7.56×10^{-2}	38.5	551	2.87×10^{-1}
109.7	37.8	103	5.37×10^{-2}	38.0	519	2.73×10^{-1}
107.8	38.9	34.9	1.81×10^{-2}	37.1	493	2.66×10^{-1}
102.8	36.2	22.9	1.24×10^{-2}	35.9	72.9	4.02×10^{-2}	35.6	382	2.18×10^{-1}
98.2	34.5	11.0	6.3×10^{-3}	35.3	322	1.94×10^{-1}
95.8	33.5	36.3	2.17×10^{-2}
93.2	31.6	223	1.44×10^{-1}
90.6	31.4	4.5	2.9×10^{-3}	31.2	24.4	1.58×10^{-2}	30.8	153	1.03×10^{-1}
88.1	30.1	3.1	2.1×10^{-3}	29.9	17.2	1.18×10^{-2}	29.2	140	9.86×10^{-2}
85.6	29.1	1.9	1.3×10^{-3}	28.8	10.8	7.7×10^{-3}
82.7	27.2	6.2	4.7×10^{-3}	26.8	54.9	4.39×10^{-2}
79.8	26.3	0.6	4.5×10^{-4}	26.0	4.0	3.3×10^{-3}
77.9	25.3	0.4	3.4×10^{-4}	24.8	1.9	1.5×10^{-3}	24.2	30.8	2.63×10^{-2}
74.3	22.8	1.2	1.1×10^{-3}	22.2	11.4	1.19×10^{-2}
70.8	20.0	9.2	1.15×10^{-2}

compound nuclei. Equation (5) is valid for a given compound nucleus in the case where all fission events occur before neutron evaporation from the compound nucleus. Because of the steepness of the excitation functions in the region of our data, we have assumed that only the first-chance fission contributes to the fission cross section. This assumption is not expected to be rigorously true, but calculations by Plasil¹¹ also indicate that the contribution to the fission cross section from latter chance fission should be small. It has also been assumed that charged-particle evaporation is a negligible mode of decay for the compound nucleus in regions where the excitation functions increase rapidly.

The total cross section for compound-nucleus formation σ_{CN} has been derived by correcting the calculated total reaction cross section σ_R for the effects of surface reaction. The ratio σ_{CN}/σ_R is taken to be 0.82, 0.80, 0.76, and 0.66 for ^{11}B , ^{12}C , ^{14}N , and ^{19}F ions, respectively.^{4,5} The remainder of the cross section is assumed to be taken up by surface reactions in which there is incomplete mo-

mentum transfer to the struck nucleus. This assumption is discussed in more detail in Ref. 5. The ratios σ_{CN}/σ_R are presumed to be independent of excitation energy.³

The ratio $\sigma_f/(\sigma_{CN} - \sigma_f)$ for the different systems studied here is plotted as a function of excitation energy in Figs. 1-3. Figure 1 also includes the curve for the system $^{169}\text{Tm} + ^{12}\text{C}$ from Ref. 3. The excitation energies were computed from the bombarding energies and the masses of the nuclei involved in the reaction. (Values for the masses were taken from Ref. 12.)

The figures show qualitatively the effect of various quantities on the fission probability. Figure 1 shows the effect of target mass on $\langle \Gamma_f/\Gamma_n \rangle$ when the same projectile is used to bombard several targets. It is observed that as Z and A of the target decreases, the excitation functions are displaced towards higher excitation energies; i.e., the fissionability decreases. A similar shift is observed with ^{16}O as the bombarding ion.³ Of special interest is the similarity of the excitation functions for ^{169}Tm and ^{174}Yb bombardments. For the compound

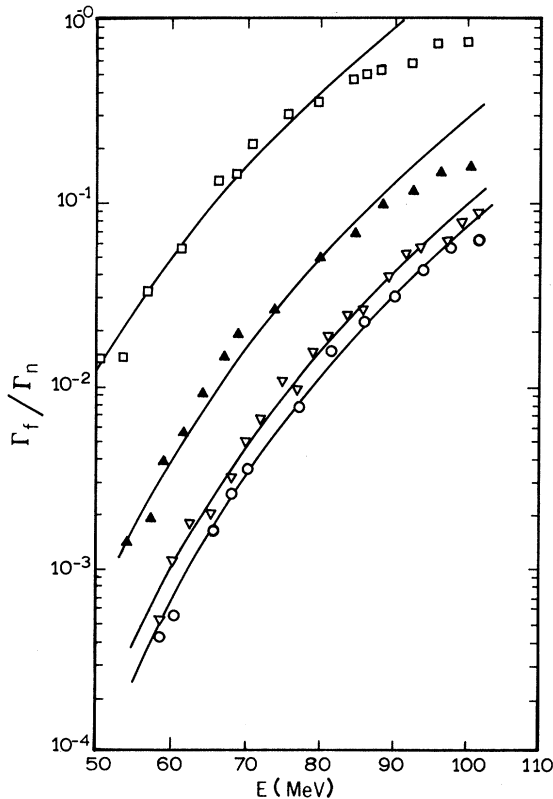


FIG. 1. Experimental $\langle \Gamma_f/\Gamma_n \rangle$ values as function of the excitation energy, E , of the compound nucleus ^{12}C incident on ^{182}W (\square); ^{175}Lu (\blacktriangle); ^{174}Yb (\circ); and ^{169}Tm (\triangle). The curves are calculated using the formula without rotational energy terms with $a_n = A/10 \text{ MeV}^{-1}$ and with the values for B'_n , a_f/a_n , and E'_f as given in Table IV.

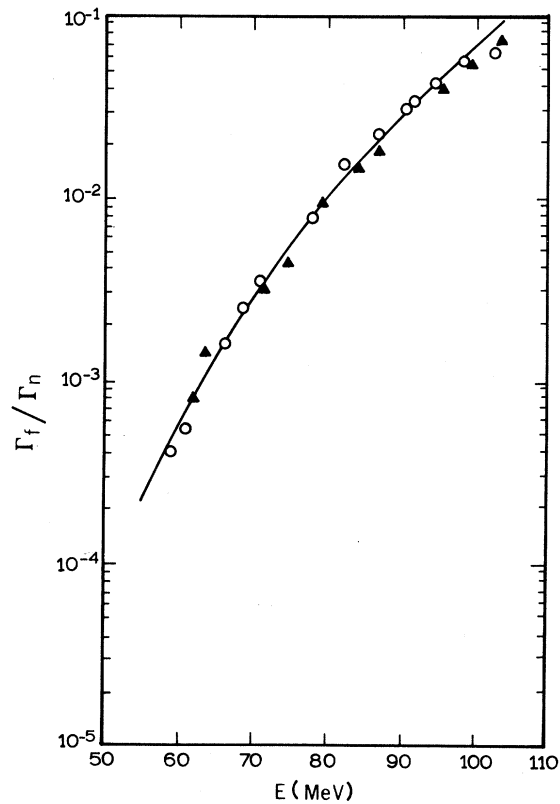


FIG. 2. Experimental $\langle \Gamma_f/\Gamma_n \rangle$ values as function of the excitation energy, E , of the compound nucleus for the reactions $^{174}\text{Yb} + ^{12}\text{C} = ^{186}\text{Os}$ (\circ) and $^{175}\text{Lu} + ^{11}\text{B} = ^{186}\text{Os}$ (\blacktriangle). The curve is calculated using the formula without rotational terms with $a_n = A/10 \text{ MeV}^{-1}$, $B'_n = 10.0 \text{ MeV}$, $a_f/a_n = 1.20$, and $E'_f = 24.7 \text{ MeV}$.

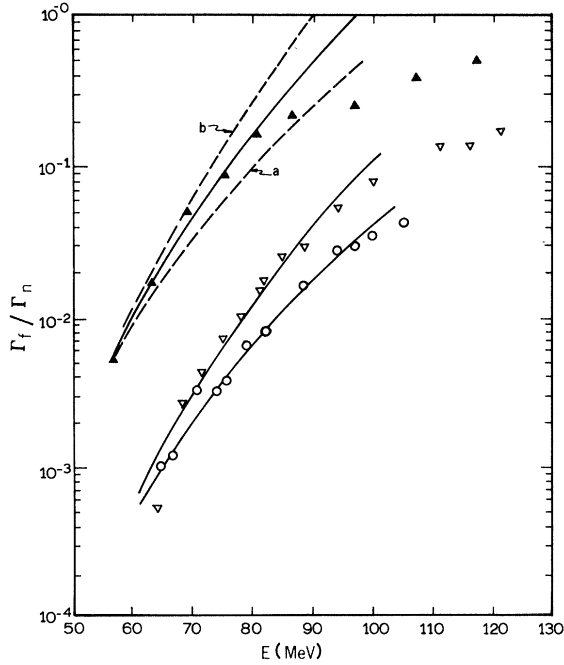


FIG. 3. Experimental $\langle \Gamma_f/\Gamma_n \rangle$ values as function of the excitation energy, E , of the compound nucleus for the reactions $^{159}\text{Tb} + ^{19}\text{F} = ^{178}\text{W}$ (\blacktriangle), $^{165}\text{Ho} + ^{14}\text{N} = ^{179}\text{W}$ (\triangle), and $^{169}\text{Tm} + ^{11}\text{B} = ^{180}\text{W}$ (\circ). The curves are calculated using the formula without rotational energy terms with $a_n = A/10 \text{ MeV}^{-1}$ and with values for B'_n as given in Table IV. For the solid lines we used the best-fit values for a_f/a_n and E'_f as listed in Table IV. For the dashed lines labeled (a) and (b), we used $a_f/a_n = 1.20$ and $E'_f = 22.4 \text{ MeV}$, and $a_f/a_n = 1.30$ and $E'_f = 24.8 \text{ MeV}$, respectively.

nuclei ^{181}Re and ^{186}Os formed in these reactions the values of the fissionability parameter Z^2/A and the neutron binding energies are very nearly the same. Hence, the expected dependence of fissionability on Z^2/A is confirmed.

From Fig. 2 it is apparent that the excitation functions for a particular compound nucleus are the same when ^{11}B and ^{12}C are used as bombarding ions. The masses of these ions are similar, resulting in approximately the same l -wave distribution for the compound nuclei formed with each of these ions. In Ref. 3 significant differences were observed between the excitation functions for the compound nucleus ^{181}Re produced by ^{12}C , ^{16}O , and ^{22}Ne ions, which give distinctly different angular momentum distributions for bombardment with each ion.

In Fig. 3 are shown the excitation functions for fission of the consecutive isotopes ^{178}W , ^{179}W , and ^{180}W . It is observed that the excitation functions for the latter two converge at low excitation energies, indicating the values of the fission barrier to be quite similar. For higher energies, the sys-

tem formed with the heaviest projectile, which involves the largest angular momentum transfer, is found to fission with the highest probability.

B. Theoretical Formula for $\langle \Gamma_f/\Gamma_n \rangle$

In the following discussion we attempt to fit theoretical $\langle \Gamma_f/\Gamma_n \rangle$ values to the experimental ones at the steep part of the curves where first-chance fission dominates. Several formulas based on statistical models exist that relate the ratio $\langle \Gamma_f/\Gamma_n \rangle$ to various nuclear quantities. A satisfactory fit to the experimental data at low energy has been obtained with one that is based on the level-density expression¹

$$\rho(E) \propto \exp[2(aE)^{1/2}] , \quad (6)$$

where angular momentum effects are included in the calculation of the energy E . For the first-chance fission we then have²

$$\begin{aligned} \langle \Gamma_f/\Gamma_n \rangle_i = & \frac{K_0 [2a_f^{1/2}(E - E'_f - E_R^f)^{1/2} - 1]}{4A^{2/3}(a_f/a_n)(E - B'_n - E_R^0)} \\ & \times \exp\{2a_n^{1/2}[(a_f/a_n)^{1/2}(E - E'_f - E_R^f)^{1/2} \\ & - (E - B'_n - E_R^0)^{1/2}]\} , \end{aligned} \quad (7)$$

and the average value of Γ_f/Γ_n is

$$\langle \Gamma_f/\Gamma_n \rangle = \left[\sum_{i=0}^{l_{\text{CN}}} \left(\frac{\Gamma_f}{\Gamma_n} \right)_i \sigma_i \right] / \sum_{i=0}^{l_{\text{CN}}} \sigma_i . \quad (8)$$

The parameters of the above equations are as follows: E - the excitation energy of the compound nucleus; σ_i - the partial cross section for the l -wave ion; $K_0 \approx 9.8 \text{ MeV}$ (Ref. 2); A - the mass number of the compound nucleus; a_n and a_f - the level-density parameters for neutron evaporation and fission, respectively; $B'_n = B_n + \Delta_n$ - the effective neutron binding energy where B_n is the neutron binding energy and Δ_n is the energy gap for the ground state of the nucleus following neutron evaporation; $E'_f = E_f + \Delta_f$ - the effective fission barrier, where E_f is the experimental fission barrier and Δ_f is the energy gap for the fissioning nucleus at the transition-state configuration; $E_R^0 = \hbar^2 l(l+1)/2\mathcal{I}_0$ - the rotational energy of the nucleus following neutron evaporation which is characterized by a moment of inertia \mathcal{I}_0 ; $E_R^f = \hbar^2 l(l+1)/2\mathcal{I}_f$ - the rotational energy of the fissioning nucleus at the transition-state shape with moment of inertia \mathcal{I}_f , and l_{CN} - a cutoff value above which compound-nucleus formation does not take place. It is estimated from the empirical relationship

$$\sigma_{\text{CN}}/\sigma_R = \left(\sum_{i=0}^{l_{\text{CN}}} \sigma_i \right) / \sum_{i=0}^{\infty} \sigma_i , \quad (9)$$

where $\sigma_{\text{CN}}/\sigma_R$ values are given in Sec. IV A.

In Eq. (7) the effect of quantum-mechanical barrier penetration has been neglected because the excitation energies spanned by the data are well above the fission barriers.¹³ We have further ignored the angular momentum carried off by a neutron, which should be a good approximation if our assumption of first-chance fission is valid. The quantities B'_n , E'_f , \mathcal{I}_0 , and \mathcal{I}_f are all functions of angular momentum since rotation is expected to alter the shapes and masses of the states which decay via neutron evaporation and fission.¹¹ We have assumed that these quantities take on the values of their nonrotating equivalents; i.e., the zero angular momentum case.

C. Fitting Procedure

As expected, good fits were obtained with many sets of values for the parameters introduced in Eqs. (7) and (8). Since the main purpose of the analysis was to extract values for E'_f , it was necessary to choose values for some of the other parameters; specifically, B'_n , a_n , and \mathcal{I}_0 , the values of which were estimated in the following way: B'_n : Values for B_n were taken from Ref. 12. The quantity Δ_n was set equal to 0, α , and 2α for an odd-odd, odd- A , and an even-even nucleus, respectively, where $\alpha = 12/\sqrt{A}$ MeV.

a_n : Values were estimated from the formula $a_n = A/10$ MeV⁻¹.

\mathcal{I}_0 : For the nucleus after neutron evaporation the moment of inertia is expected to be very nearly equal to the moment of inertia of a rigid body. We have assumed the shape of this state to be spherical so that

$$\mathcal{I}_0 = \frac{2}{5} m r_0^2 A^{5/3},$$

where m is one atomic-mass unit and $r_0 = 1.22 \times 10^{-13}$ cm is the nuclear radius parameter.

The uncertainty in B'_n is about 2 MeV which will introduce a similar error in E'_f . The parameters a_n and \mathcal{I}_0 are weakly correlated with the other parameters, e.g., E'_f , a_f/a_n , and $\mathcal{I}_f/\mathcal{I}_0$ (see Refs. 3 and 14). Hence, the functional forms of a_n and \mathcal{I}_0 are not critical. We shall in the evaluation of the errors in E'_f , assign an uncertainty of 10 units in a_n . In the fitting process we found that the slope of $\langle \Gamma_f/\Gamma_n \rangle$ increases strongly when the values of a_f/a_n and $\mathcal{I}_f/\mathcal{I}_n$ were, respectively, increased or decreased. Their values could both be chosen as constants independent of excitation energy, and of target and ion used. The result of such an analysis is presented below in Sec. IV E. Most importantly, if a_f/a_n indeed is a constant, the rotational energy terms in Eq. (7) cannot be left out if one is to obtain a fit to the data. When these terms are ignored one obtains, however, equally good fits if

a_f/a_n is allowed to be a function of the target and ion. In this case the angular momentum effects are tied in with the value of a_f/a_n . The advantage of such a procedure is that one does not have to know the angular momentum distribution of the compound nucleus. The results of such an approach is presented in the following.

D. Level-Density Formula Without Rotational Energy Terms

In this case we have taken E'_f and a_f/a_n as the only adjustable parameters, both of which are assumed to be independent of bombarding energy. Their best-fit values for the various systems are given in Table IV and the corresponding calculated $\langle \Gamma_f/\Gamma_n \rangle$ values are presented as curves in Figs. 1-3. We see that the fit to experimental values is excellent for the onset of the excitation function. In Fig. 3 are also shown the curves which represent the limits of what we define as a reasonable fit. This introduced errors of only 0.05 and 1.0 MeV in a_f/a_n and E'_f , respectively. Their over-all errors were 0.10 and 4.0 MeV, respectively, when the errors of 2 MeV in B'_n and 10 MeV⁻¹ in a_n were taken into account.

The data in Table IV show that within the limits of our errors a_f/a_n is independent of the target used and increases with increasing mass of the ion. This is a direct result of angular momentum effects. That is, the average angular momentum and hence $\langle \Gamma_f/\Gamma_n \rangle$ increase faster with excitation energy as the mass of the ion increases. Assuming a linear variation of a_f/a_n with the projectile mass number A_i , of the ion, we obtain the following empirical relationship:

$$a_f/a_n = 1.11 + 0.075A_i. \quad (10)$$

Hence, for a nonrotating system the value of a_f/a_n is 1.11 which should correspond to the one obtained using the formula containing rotational energy terms. It is difficult to attach physical significance to such an expression. However, such a semiempirical expression has considerable utility for prediction purposes.

E. Level-Density Formula with Rotational Energy Terms

The best over-all fit to the data was obtained with the values 1.20 and 2.0 for the ratios a_f/a_n and $\mathcal{I}_f/\mathcal{I}_0$, respectively. These values are in agreement with previous results.³ The values for E'_f are listed in Table IV and the calculated curves for $\langle \Gamma_f/\Gamma_n \rangle$ were similar to those given in Figs. 1-3. The over-all error in a_f/a_n was estimated to be 0.05. This quantity is correlated strongly with E'_f but rather weakly with a_n , the ratio $\mathcal{I}_f/\mathcal{I}_0$,

TABLE IV. Various quantities used in the fit of calculated $\langle \Gamma_f / \Gamma_n \rangle$ values to experimental ones, and a comparison of experimental and calculated fission-barrier values.

System	Compound nucleus	Z^2/A	B_n' (MeV)	a_f/a_n ^a	E_f' ^a (MeV)	E_f' ^b (MeV)	E_f ^c (MeV)
$^{159}\text{Tb} + ^{19}\text{F}$	^{178}W	30.76	10.7	1.25	21.5	23.0	25.3 ^d
$^{165}\text{Ho} + ^{14}\text{N}$	^{179}W	30.59	7.5	1.24	23.2	25.2	25.6 ^d
$^{169}\text{Tm} + ^{11}\text{B}$	^{180}W	30.42	10.3	1.19	25.0	28.7	25.0
$^{169}\text{Tm} + ^{12}\text{C}$	^{181}Re	31.08	9.7	1.21	24.0	25.0 ^e	23.9 ^d
$^{174}\text{Yb} + ^{12}\text{C}$	^{186}Os	31.05	10.0	1.20	24.7	25.7	23.2
$^{175}\text{Lu} + ^{11}\text{B}$	^{186}Os	31.05	10.0	1.20	24.9	26.0	23.2
$^{175}\text{Lu} + ^{12}\text{C}$	^{187}Ir	31.71	9.4	1.20	21.6	21.8	21.1
$^{182}\text{W} + ^{12}\text{C}$	^{194}Hg	32.99	10.2	1.20	19.8	19.4	18.3

^aBest-fit values when $a_n = A/10 \text{ MeV}^{-1}$ and rotational energy terms are ignored.

^bBest-fit values when $a_n = A/10 \text{ MeV}^{-1}$, $a_f/a_n = 1.20$, and $g_f/g_0 = 2.0$.

^cValues taken from Ref. 15.

^dThis value is equal to that of the saddle mass, as taken from Ref. 15, reduced by 1.0 MeV.

^eData taken from Ref. 3.

and the angular momentum distribution, including its variation with excitation energy. The reason for the weak correlation in the latter two cases is that the average values for E_R^0 and E_R^f are much smaller than those for E_f' . This introduces, however, a large error in g_f/g_0 . For the assumed l distribution we find this error to be about 0.5. The formula we have used to estimate the l distribution is semiempirical and contains several parameters whose values have been obtained by extrapolation. The reliability of this cannot be evaluated. The errors in the values for the parameters E_L , a_f/a_n , g_f/g_0 , B_n' , and a_n introduce in E_f' the errors 2.0, 1.5, and 1.2, 2.0, and 0.8 MeV, respectively, to a combined uncertainty of about ± 3.5 MeV for E_f' .

V. CONCLUSION

The data in Table IV suggest that the average values for E_f' and a_f/a_n are, respectively, only about 1.5 MeV lower and 0.02 higher when the formula without rotational energy terms is used. In Table IV we have also listed the values for E_f as estimated by Myers and Swiatecki using a semiempirical formula.¹⁵ The agreement is quite consistent with the predictions of Ref. 15. It is interesting to note

that the average difference between the values of E_f and E_f' corresponds to a value of 0.7 and 1.4 MeV for the energy gap at saddle of an odd- A and an even-even nucleus, respectively. However, the uncertainty in the data is too large to take these values for the energy gap seriously. A linear extrapolation of the values for a_f/a_n given in Table IV yields a value of 1.11 for a_f/a_n for a nonrotating system. This is substantially lower than the value of 1.20 obtained with the formula which contains rotational energy terms. Since we do not know if such a linear extrapolation is justified we suggest rather conservatively that in this region of the Periodic Table the value of a_f/a_n is 1.20 ± 0.10 .

Our conclusion is that when E_f' is large the inclusion or exclusion of rotational energy terms in the formula for $\langle \Gamma_f / \Gamma_n \rangle$ yields similar values for E_f' and a_f/a_n . The latter analysis is rather easy to perform. We should finally reemphasize that the fits have been made only at the lowest energies of the excitation functions. As the energy increases the deviation between calculated and experimental $\langle \Gamma_f / \Gamma_n \rangle$ values increases. Possible reasons for this discrepancy have been discussed in Ref. 3.

*Work done under the auspices of the U. S. Atomic Energy Commission.

†Permanent address: Institute of Physics, University of Trondheim-NTH, Trondheim, Norway.

‡Permanent address: Lawrence Radiation Laboratory, University of California, Livermore, California.

§Permanent address: Department of Nuclear Science, Israel Institute of Technology, Haifa, Israel.

||Permanent address: Chemistry Department, University of Maryland, College Park, Maryland.

¹E. K. Hyde, I. Perlman, and G. T. Seaborg, *The Nuclear Properties of the Heaviest Elements III, Fission Phenomena* (Prentice-Hall, Englewood Cliffs, New Jersey, 1964), pp. 298 and 383.

²J. R. Huizenga and R. Vandenbosch, in *Nuclear Reactions*, edited by P. M. Endt and P. B. Smith (North-Holland Publishing Company, Amsterdam, The Netherlands, 1962), Vol. II.

³T. Sikkeland, Phys. Rev. **135**, B669 (1964).

⁴T. Sikkeland, E. L. Haines, and V. E. Viola, Jr.,

Phys. Rev. **125**, 1350 (1962).

⁵T. Sikkeland and V. E. Viola, Jr., in *Proceedings of the Third International Conference on Reactions Between Complex Nuclei, Asilomar, 14-18 April 1963*, edited by A. Ghiorso, R. M. Diamond, and H. E. Conzett (University of California Press, Berkeley, California, 1963).

⁶L. C. Northcliffe, Phys. Rev. **120**, 1744 (1960).

⁷H. H. Heckman, B. L. Perkins, W. G. Simon, F. M. Smith, and W. H. Barkas, Phys. Rev. **117**, 544 (1960).

⁸W. G. Simon, H. H. Heckman, and E. L. Hubbard, in *Proceedings of the Second International Conference on the Physics of Electronic and Atomic Collisions* (W. A. Benjamin, Inc., New York, 1961), p. 80.

⁹T. D. Thomas, Phys. Rev. **116**, 703 (1959).

¹⁰V. E. Viola, Jr., and T. Sikkeland, Phys. Rev. **128**, 767 (1962).

¹¹F. Plasil, Lawrence Radiation Laboratory Report No. UCRL-11193, 1963 (unpublished).

¹²The masses of all projectiles were taken from the experimental mass tables of J. H. E. Mattauch, W. Thiele, and A. H. Wapstra, Nucl. Phys. **67**, 1 (1965); all target masses and masses for the compound nuclei ¹⁷⁸W, ¹⁸⁰W, ¹⁸⁶Os, and ¹⁹⁴Hg were taken from the experimental mass tables of S. Liran and N. Zeldes, Nucl. Phys. **A136**, 190 (1969); masses for the compound nuclei ¹⁷⁹W, ¹⁸¹Re, and ¹⁸⁷Ir were taken from the semiempirical mass calculations of N. Zeldes, M. Gronau, and A. Lev, Nucl. Phys. **63**, 1 (1965).

¹³J. R. Huizenga, R. Chaudry, and R. Vandenbosch, Phys. Rev. **126**, 210 (1962).

¹⁴D. S. Burnett, R. G. Gatti, F. Plasil, P. B. Price, W. F. Swiatecki, and S. G. Thompson, Phys. Rev. **134**, B952 (1964).

¹⁵W. Myers and W. F. Swiatecki, Nucl. Phys. **81**, 1 (1966).

PHYSICAL REVIEW C

VOLUME 3, NUMBER 1

JANUARY 1971

Ru^{103, 105} States Observed in the Reactions Ru^{102, 104}(*d, p*)[†]

H. T. Fortune,* G. C. Morrison, J. A. Nolen, Jr.‡
Argonne National Laboratory, Argonne, Illinois 60439

and

P. Kienle§
Argonne National Laboratory, Argonne, Illinois 60439
and Physik Department der Technischen Hochschule Munich, Munich, Germany
(Received 1 October 1970)

The (*d, p*) reaction on Ru¹⁰² and Ru¹⁰⁴ has been studied at an incident deuteron energy of 14 MeV. Proton spectra were recorded in a broad-range magnetic spectrograph. Transferred *l* values and spectroscopic factors were obtained by comparing the measured angular distributions with distorted-wave Born-approximation predictions. The low-lying levels of Ru¹⁰³ are in good agreement with the results of a recent (*d, t*) study; information on higher levels of Ru¹⁰³ and on all levels in Ru¹⁰⁵ is new. There is good correspondence between strongly excited levels in the two isotopes, although there is evidence of a higher level density in Ru¹⁰⁵. The summed spectroscopic factors give information on the extent of filling of the neutron orbitals in the targets, and these results are in reasonable agreement with results from the (*d, t*) reaction and for other nuclei in this region.

I. INTRODUCTION

It has been suggested¹ that stable quadrupole deformations may occur in nuclei with $40 < Z < 50$ and with $N > 60$. This includes the region of neutron-rich Mo, Ru, and Pd isotopes. Support for this suggestion comes from the fact that the energies of the first excited 2⁺ states in such even-even isotopes decrease appreciably as neutrons are added; this feature is most pronounced in the Ru isotopes. Further support comes from the mass dependence of delayed γ -ray yields from fission fragments²; again the heavy Ru isotopes appear to be the most likely region in which to find nuclei with low-lying deformed states.

Almost all of the experimental evidence on deformation involves the study of complex γ -ray transitions, and rarely can the level structure be uniquely determined from such data alone. A particularly complex spectrum was observed³ in the decay of Tc¹⁰⁵ to Ru¹⁰⁵. In order to gain spectroscopic information on the level structure of nuclei in this region, we have studied (*d, p*) reactions on the most neutron-rich stable Ru¹⁰² and Ru¹⁰⁴ targets. Of special interest was the comparison between the level structures of the two nuclei in an effort to obtain evidence for or against a change in character between Ru¹⁰³ and Ru¹⁰⁵.

Also of interest is the comparison between the results for these Ru isotopes and the correspond-